



Full length article

Water geochemistry of rivers draining karst-dominated regions, Guangxi province, South China: Implications for chemical weathering and role of sulfuric acid



Hao Jiang^{a,c,d}, Wenjing Liu^{a,b,c,d}, Tong Zhao^{a,c,d}, Huiguo Sun^{a,c,d}, Zhifang Xu^{a,b,c,d,*}

^a Key Laboratory of Cenozoic Geology and Environment, Institute of Geology and Geophysics, Chinese Academy of Sciences, Beijing 100029, China

^b CAS Center for Excellence in Life and Paleoenvironment, Beijing 100044, China

^c Institutions of Earth Sciences, Chinese Academy of Sciences, Beijing 100029, China

^d University of Chinese Academy of Sciences, Beijing 100049, China

ARTICLE INFO

Keywords:

Water chemistry
Chemical weathering
Sulfuric acid
CO₂ budget

ABSTRACT

Guangxi province, located in South China, is a typical karst region affected by acid depositions for a couple of decades. Water samples from the major river basins in this region were collected and the chemical compositions were measured with a main purpose to quantify chemical weathering rates and associated CO₂ budget. The average total dissolved solids (TDS) of the river waters (232 mg/l) are comparable with other karstic rivers. The major ion compositions of the river waters are characterized by the dominance of Ca²⁺, Mg²⁺, HCO₃⁻, and are significantly rich in SO₄²⁻. The chemical compositions of the river waters indicate that four major reservoirs (atmospheric, anthropogenic, carbonate and silicate inputs) contribute to the dissolved loads. The carbonate chemical weathering rates range from 61.4 t/km²/yr for the Qingshuihe river basin to 93.3 t/km²/yr for the Zuojiang river basin. The silicate chemical weathering rates range from 2.9 t/km²/yr for the Qingshuihe river basin to 7.9 t/km²/yr for the Liujiang river basin. The CO₂ consumption rates by carbonate weathering range from 559 × 10³ mol/km²/yr for the Qingshuihe river basin to 817 × 10³ mol/km²/yr for the Zuojiang river basin. The CO₂ consumption rates by silicate weathering range from 19 × 10³ mol/km²/yr for the Zuojiang river basin to 85 × 10³ mol/km²/yr for the Liujiang river basin. Sulfuric acid is involved as a proton donor in weathering reactions, and about 9–15% of the chemical weathering rates of the river basins are sulfuric acid-induced. The CO₂ consumption rates are only 85–91% of the value when assuming carbonic acid provides all the protons in the weathering reactions. The CO₂ released from sulfuric acid-induced carbonate weathering would exceed the CO₂ consumed by silicate weathering, making the river basins in Guangxi net CO₂ sources on geological timescales. The total net CO₂ releasing flux is approximately 15.7 × 10⁹ mol/yr (0.19 × 10¹² gC/yr). This result quantitatively highlights the fact that CO₂ budget by chemical weathering will be largely modified by sulfuric acid, especially in seriously acid deposition affected region.

1. Introduction

The global carbon cycle of the Earth is the most critical factor regulating the long-term evolution of global climate. The key idea of today's carbon cycle models is that Earth sequesters CO₂ released from Earth's interior, thus preventing it from being released into the atmosphere and causing warming (Bernier and Kothavala, 2001; Wallmann, 2001; Gaillardet and Galy, 2008). Continental chemical weathering is one of the main sequestering processes. Many studies have estimated chemical weathering rates and associated CO₂ consumption rates of basin or global scales using chemical fluxes of rivers (e.g. Gaillardet et al., 1999; Galy and France-Lanord, 1999; Millot et al.,

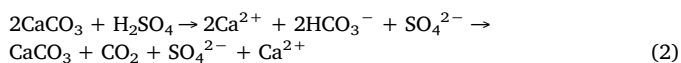
2003; Moon et al., 2007, 2014; Wu et al., 2008; Noh et al., 2009; Xu and Liu, 2010; Li et al., 2014; Liu et al., 2016; Wu, 2016). Chemical weathering of silicates is recognized as the dominant long-term sink for atmospheric CO₂ whereas chemical weathering of carbonates is thought to be ineffective because the CO₂ consumed is supposed to be balanced by the CO₂ released to the atmosphere through carbonate precipitation in the ocean (Eq. (1)) (Walker et al., 1981; Bernier et al., 1983; Bernier, 1991).



However, the carbonate sub-cycle mentioned above only considered

* Corresponding author at: Key Laboratory of Cenozoic Geology and Environment, Institute of Geology and Geophysics, Chinese Academy of Sciences, Beijing 100029, China.
E-mail address: zfxu@mail.iggcas.ac.cn (Z. Xu).

CO₂ as the unique weathering agent. Sulfuric acid from sulfides oxidation and acid deposition may also provide the required proton. Equation of carbonate sub-cycle involving sulfuric acid is:



On the one hand, chemical weathering of carbonate rocks by sulfuric acid might be a transient source of CO₂ to the atmosphere instead of CO₂ sequestration because the longer residence time of sulfate (10⁷ yrs) compared to that of carbonate ions (10⁵ to 10⁶ yrs) in the ocean (Hercod et al., 1998; Galy and France-Lanord, 1999; Yoshimura et al., 2001; Spence and Telmer, 2005; Calmels et al., 2007; Li et al., 2008, 2014). On the other hand, the drawdown of CO₂ by silicate weathering would be overestimated when sulfuric acid-induced chemical weathering is ignored (Spence and Telmer, 2005; Liu et al., 2016). With increasing disturbance of human activity, acid deposition may play a significant role in chemical weathering processes (Amiotte-Suchet et al., 1995; Probst et al., 2000; Lerman et al., 2007; Li et al., 2008; Pacheco et al., 2013; Liu et al., 2016). On a global scale, the CO₂ consumption by weathering was decreased by approximately 13% due to sulfuric acid deposition (Amiotte-Suchet et al., 1995; Liu et al., 2016). Therefore, systematic study is needed to ascertain the role of sulfuric acid in chemical weathering, which is essential for the accurate estimation of carbon source and sink (Moon et al., 2007; Chetelat et al., 2008; Kashiwagi et al., 2008; Torres et al., 2014, 2016).

Studies have reported the water geochemistry and chemical weathering processes of the Xijiang river basin based on time-series samples collected at hydrological stations (Zhang et al., 2007; Gao et al., 2009; Wei et al., 2013) and samples collected at the mainstream and the main tributaries (Xu and Liu, 2010). Xu and Liu (2007) and Li et al. (2008) reported the chemical weathering processes as well as the important role of sulfuric acid in the Nanpanjiang and the Beipanjiang river basins, the two headwater basins of the Xijiang river basin. However, the weathering processes of the river basins in Guangxi, the middle reaches of the Xijiang river, has not been systematically studied. Guangxi is one of the most typical karst region in the world, with a large continuous exposure area of carbonate rocks (about 90,000 km²), and is also one of the most seriously acid deposition affected region in South China. Therefore, it is an ideal setting to investigate the role of sulfuric acid in chemical weathering of carbonates. In this study, we carried out a systematic investigation on the elemental compositions of river waters from the river basins in Guangxi. One aim of this study is to calculate the silicate and carbonate weathering rates as well as the associated CO₂ consumption rates. Another aim is to evaluate the role of sulfuric acid in the chemical weathering processes in a typical acid rain effected karstic region in South China. The disturbance of sulfuric acid from natural source and anthropogenic source to the local CO₂ budget is discussed separately.

2. Natural settings of the study area

Guangxi province is located in the southern part of China, lying between 20°54′ and 26°24′N latitude and between 104°26′ and 112°4′E longitude, with an area of 2.37 × 10⁵ km². It is bordered by Yunnan to the west, Guizhou to the north, Hunan to the northeast, Guangdong to the east and southeast, and also bordered by Vietnam to the southwest. The rivers in Guangxi belong mainly to the Xijiang river system (Fig. 1). The Yujiang river is the largest tributary of the Xijiang river, with a total length of 1179 km, drainage area of 89,870 km², and average annual discharge of 502 × 10⁸ m³/y. The Zuojiang river and the Youjiang river are the two headwater tributaries of the Yujiang river, with total lengths of 539 and 707 km, drainage areas of 32,068 and 38,612 km², and average annual discharge of 174 × 10⁸ m³/y and 145 × 10⁸ m³/y, respectively. The Liujiang river is the second largest tributary of the Xijiang river, with a total length of 773 km, drainage area

of 58,270 km², and average annual discharge of 527 × 10⁸ m³/y. The Xijiang river flows into Guangxi province at Tian'e with average annual discharge of 510 × 10⁸ m³/y, and finally flows out at Wuzhou, with average annual discharge of 2200 × 10⁸ m³/y. The elevation gradients of the river basins in Guangxi are abrupt, with the altitudes decrease from 1800 m at the upper reaches of the rivers to 30 m at the lower reaches.

Guangxi is subject to a subtropical monsoon climate, with mean annual precipitation of 1500–2000 mm and mean annual temperature of 16.5–23.1 °C. Anthropogenic pressure is considerable as about 46 million people live in Guangxi, with a density of about 190 persons per km². The region has been characterized by high rate of acid deposition for a couple of decades caused by SO₂ emissions associated with coal combustion (Wang and Wang, 1996; Larssen et al., 1999). It is estimated that the S emissions rate to the atmosphere is about 5.1 × 10⁵ t/y and the S deposition rate is about 3.1 × 10⁵ to 3.8 × 10⁵ t/y (Wang et al., 2000; Xu et al., 2006).

Guangxi is a typical karst region, with the central part of the region constituting a land of karst hills and plains. Lithologically, it consists of rocks from Precambrian metamorphic rocks to Quaternary fluvial sediments. The Triassic, Permian, Carboniferous and Devonian carbonate rocks (limestone and dolomite) is mainly distributed in the central part of Guangxi (Fig. 1). The thickness of carbonate rock strata is more than ten thousand meters (Yuan, 1991). Sedimentary rocks and coal-bearing formations are widely distributed in Guangxi and the coal deposits are rich in sulfides (Xu and Liu, 2007; Gao et al., 2009; Xu and Liu, 2010). Precambrian metamorphic rocks (schist and slate) and igneous rocks (mainly granite) are mainly distributed in the northern and eastern part of Guangxi, respectively. Evaporites were rare to be described in the region by geological surveys (Geological Bureau of Guangxi Zhuang Autonomous Region, 1985).

3. Sampling and analytical procedures

Water samples from the river basins in Guangxi were collected during high-flow season in June 2012. The sampling locations are shown in Fig. 1. The river water samples were collected near the middle of the flow (approximately 10–20 cm depth from the river surface) using 10 L high density polyethylene (HDPE) containers and immediately filtered through 0.22 μm Millipore mixed cellulose esters membrane filters. Two aliquots were prepared: one aliquot of the filtered water was acidified with double sub-boiling distilled HNO₃ (6 M) to pH < 1.6 and stored in a polyethylene bottle for cations analyses and another was stored directly in a polyethylene bottle for anion analyses. All containers were previously washed with Millipore-Q purified water (18.2 MΩ) and rinsed with river water twice before the actual sampling (Xu and Liu, 2010).

The water temperature (T), pH and electric conductivity (EC) were measured in the field using a portable EC/pH meter (YSI-6920, USA). The alkalinity was determined using a titration method within 12 hours after sampling. Major cations (Na⁺, K⁺, Ca²⁺ and Mg²⁺) were analyzed by Atomic Absorption Spectrometry (AAS) with a detection limit of 0.1 ppm and a precision of ± 3%. Anions (Cl⁻, SO₄²⁻ and NO₃⁻) were analyzed by Ion Chromatography (Dionex 120, USA) with a detection limit of 0.1 ppm and a precision of ± 5%. The dissolved SiO₂ concentrations were determined using the molybdate blue method by spectrophotometry. Procedural and reagent blanks were determined along with the sample treatment. Each calibration curve was evaluated by analyses of the quality control standards before and after the analyses of a set of samples. The saturation state index with regards to calcite (SIC) was calculated using the PHREEQC program.

4. Results

The pH, T, EC, major ions, dissolved SiO₂ in the river waters are given in Table 1. The average pH of the samples is 7.8, ranging from 6.5

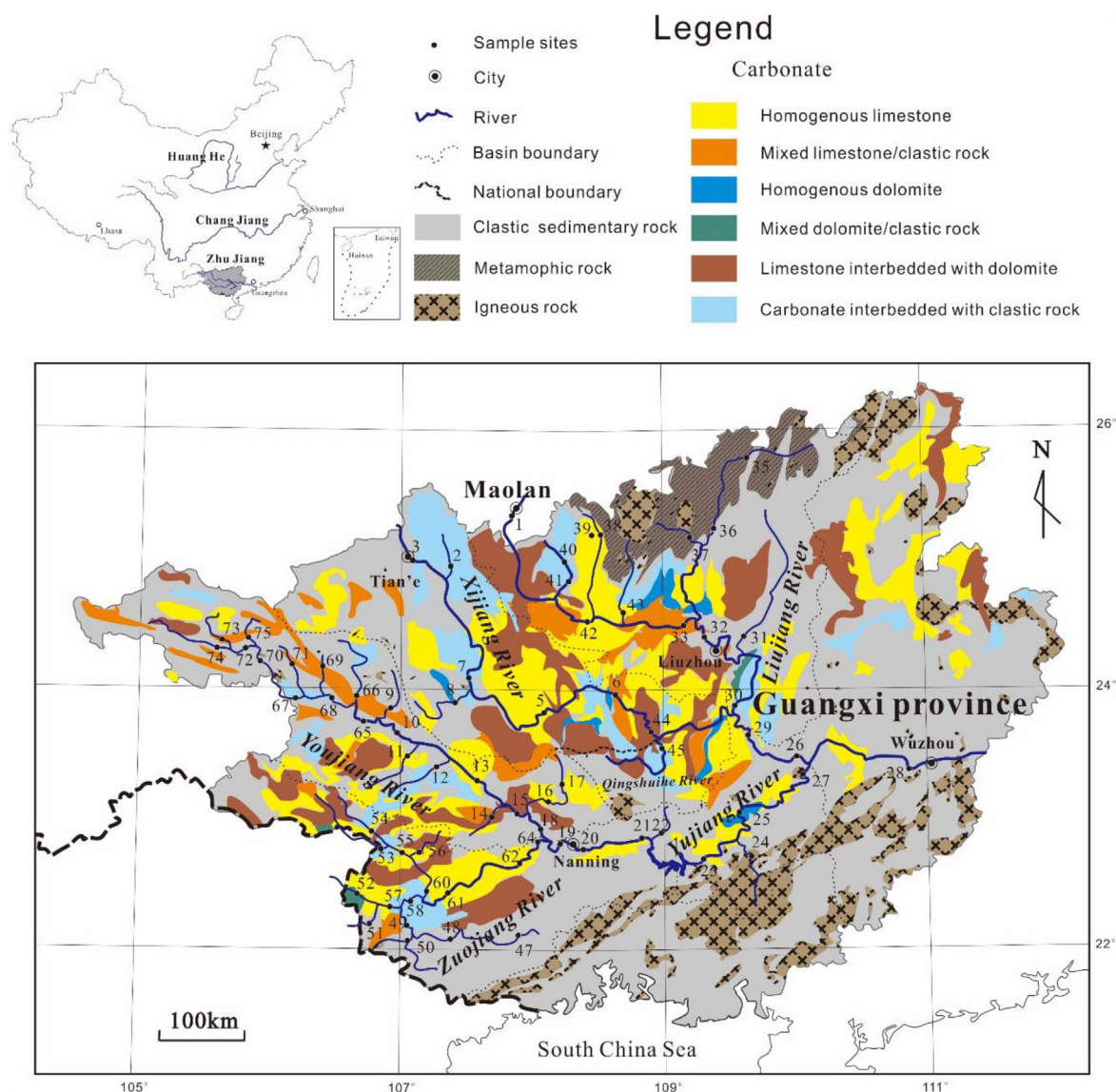


Fig. 1. Sketch map showing the lithology of Guangxi province and the sampling locations of the river waters.

to 8.5. The average conductivity is 262 $\mu\text{S}/\text{cm}$, ranging from 25 to 384 $\mu\text{S}/\text{cm}$. The normalized inorganic charge balance (NICB = $(\text{TZ}^+ - \text{TZ}^-)/\text{TZ}^+$, where $\text{TZ}^+ = \text{Na}^+ + \text{K}^+ + 2\text{Mg}^{2+} + 2\text{Ca}^{2+}$ and $\text{TZ}^- = \text{Cl}^- + 2\text{SO}_4^{2-} + \text{HCO}_3^-$, in 10^{-6} charge equivalent units per liter), is generally less than 10%, which indicates that unanalyzed organic anions are only a minor component. The total dissolved solid (TDS) of the samples varies from 29 to 351 mg/l, with an average of 232 mg/l, which is comparable with the Wujiang, the Yuanjiang, the Hanjiang, the Panjiang, the Yalongjiang and the Xijiang rivers draining carbonate-dominated regions in China (Han and Liu, 2004; Xu and Liu, 2007; Zhang et al., 2007; Li et al., 2008; Li and Zhang, 2008; Gao et al., 2009; Han et al., 2010a; Xu et al., 2011; Li et al., 2014).

Variations of major ion compositions are shown in the cation and anion ternary diagram (Fig. 2). Most of the samples cluster toward the Ca^{2+} apex (Fig. 2a), and HCO_3^- apex (Fig. 2b). Ca^{2+} and Mg^{2+} account for 80–96% (averaging at 90%) of the total cations and HCO_3^- accounts for 50–92% (averaging at 83%) of the total anions. SO_4^{2-} is next most abundant anion after HCO_3^- , which accounts for about 10% of the total anions. The samples contain relatively low concentrations of Cl^- , NO_3^- , K^+ , Na^+ and SiO_2 . A few samples collected at the upper reaches of the Liujiang river have distinctly higher proportions of SiO_2 , K^+ and Na^+ and low TDS values. The dominance of Ca^{2+} , Mg^{2+} and

HCO_3^- , with SO_4^{2-} also being enriched, represents the typical characteristics of the major ion compositions of the river waters. No significant seasonal variation of elemental concentrations was observed in previous studies (Gao et al., 2009; Wang et al., 2012; Wei et al., 2013). The SIC of the samples is generally above 0, except for those draining metamorphic and igneous regions (e.g. samples 26, 36 and 37), indicating that most of the samples are supersaturated with regards to calcite.

5. Discussions

5.1. Sources of solutes

The dissolved loads of river water are generally the products of chemical weathering of rocks, atmospheric deposition and anthropogenic inputs. To calculate the chemical weathering rates and associated CO_2 consumption rates of the river basins, it is necessary to constrain the contributions of the different sources to the major ion budgets.

5.1.1. Atmospheric inputs

Chloride (Cl^-) is the most useful reference to evaluate atmospheric

Table 1
Chemical compositions of the river water samples from the river basins in Guangxi, South China.

Sample number	Rivers	Date	pH	EC	T	HCO ₃ ⁻	F ⁻	Cl ⁻	NO ₃ ⁻	SO ₄ ²⁻	SiO ₂	K ⁺	Na ⁺	Ca ²⁺	Mg ²⁺	TZ ⁺	TZ ⁻	NICB ^a	TDS	Slc
		(y/m/d)		μS/cm	°C	μmol/l										μeq		%	mg/l	
<i>Xijiang River (Mainstream)</i>																				
2	XJ-1	2012/06/13	7.98	265	24.8	1850	3	38	100	347	96	30	53	1189	128	2717	2684	1.2	213	0.3
3	XJ-2	2012/06/13	7.66	164	22.1	2800	4	94	128	452	57	41	228	1471	389	3989	3929	1.5	304	0.2
5	XJ-3	2012/06/14	7.82	341	23.1	2820	4	79	113	350	62	35	178	1452	320	3757	3715	1.1	291	0.4
6	XJ-4	2012/06/14	7.85	330	22.1	2710	4	76	109	335	2	35	180	1411	311	3659	3570	2.4	277	0.3
7	XJ-5	2012/06/14	7.87	329	22.6	2710	3	77	110	338	70	35	184	1432	316	3716	3575	3.8	282	0.4
8	XJ-6	2012/06/14	8.09	208	26.5	1870	2	63	100	55	164	30	125	932	101	2221	2143	3.5	181	0.3
26	XJ-7	2012/06/18	7.92	285	24.9	2410	2	78	126	219	80	31	116	1259	238	3141	3054	3.0	244	-1.4
28	XJ-8	2012/06/18	7.76	284	27.3	2350	1	105	140	198	83	43	126	1226	220	3063	2993	2.3	239	0.2
29	XJ-9	2012/06/18	7.72	258	25.0	2380	4	79	127	222	81	31	123	1247	243	3134	3034	3.2	242	0.2
44	XJ-10	2012/06/21	7.84	340	24.4	2890	3	95	144	364	68	35	160	1602	318	4035	3861	4.3	305	0.4
<i>Liujiang River</i>																				
1	LJ-1	2012/06/13	7.91	310	20.9	2410	2	54	94	277	71	23	48	1181	359	3153	3112	1.3	244	0.3
30	LJ-2	2012/06/19	7.90	199	25.9	1540	3	66	112	142	102	28	101	805	186	2112	2005	5.1	163	0.0
31	LJ-3	2012/06/19	7.87	163	28.0	1300	1	74	100	76	89	26	89	658	154	1737	1626	6.4	134	-0.2
32	LJ-4	2012/06/19	7.73	181	26.2	1430	0	52	90	126	112	23	101	724	174	1920	1824	5.0	150	-0.2
33	LJ-5	2012/06/19	7.97	326	25.6	2820	2	67	129	249	82	25	72	1493	295	3673	3517	4.2	281	0.5
35	LJ-6	2012/06/19	7.51	54	25.1	408	0	27	28	39	128	14	94	151	69	548	542	1.0	49	-0.2
36	LJ-7	2012/06/20	7.06	59	24.5	408	1	34	38	52	141	18	140	162	70	623	585	6.0	54	-2.1
37	LJ-8	2012/06/20	7.14	25	24.4	168	1	24	39	20	125	20	91	59	30	289	273	5.7	29	-2.8
38	LJ-9	2012/06/20	7.82	164	26.1	1310	1	32	32	161	113	12	88	548	282	1758	1697	3.5	137	-0.3
39	LJ-10	2012/06/20	7.43	310	24.6	1930	0	42	50	731	78	17	53	1343	345	3446	3483	-1.1	261	-0.2
40	LJ-11	2012/06/20	8.14	346	26.0	2510	0	54	52	614	41	17	160	1500	422	4022	3843	4.4	294	0.6
41	LJ-12	2012/06/20	7.77	339	26.0	2440	1	58	71	675	70	18	72	1543	394	3965	3920	1.1	298	0.3
42	LJ-13	2012/06/20	7.74	346	24.4	3040	1	68	134	357	71	22	63	1715	303	4122	3957	4.0	313	0.4
43	LJ-14	2012/06/20	7.79	227	25.7	2070	1	47	77	131	97	19	71	1028	251	2646	2458	7.1	201	0.1
<i>Yujiang River</i>																				
19	YuJ-1	2012/06/16	7.67	306	28.1	2640	2	121	160	161	90	44	144	1380	202	3352	3245	3.2	261	0.2
20	YuJ-2	2012/06/16	7.73	221	29.9	1660	8	249	81	84	91	90	324	764	193	2327	2164	7.0	175	-0.1
21	YuJ-3	2012/06/17	7.88	310	28.0	2730	3	117	79	164	92	50	177	1385	203	3404	3257	4.3	263	0.5
22	YuJ-4	2012/06/17	7.82	209	29.6	1420	6	200	177	88	107	80	153	672	282	2141	1979	7.5	160	-0.1
23	YuJ-5	2012/06/17	7.77	308	28.7	2540	3	164	183	163	89	59	205	1352	205	3377	3216	4.8	259	0.3
24	YuJ-6	2012/06/17	7.53	111	28.2	786	4	77	73	53	172	84	198	342	79	1124	1045	7.0	94	-1.0
25	YuJ-7	2012/06/18	7.80	282	28.2	2290	3	162	165	153	94	65	211	1206	186	3059	2925	4.4	236	0.3
27	YuJ-8	2012/06/18	7.72	269	29.7	2090	2	170	171	154	89	71	182	1123	180	2858	2740	4.1	220	0.1
<i>Zuojiang River</i>																				
47	ZJ-1	2012/06/22	6.47	33	25.1	204	0	54	11	33	56	26	51	116	26	361	336	7.0	29	-3.1
49	ZJ-2	2012/06/22	7.49	91	25.7	528	3	155	86	54	92	44	109	306	86	937	880	6.0	72	-1.2
50	ZJ-3	2012/06/22	8.02	275	25.1	2280	4	330	78	125	162	96	315	1230	165	3199	2942	8.0	242	0.4
51	ZJ-4	2012/06/23	7.86	162	29.5	1395	1	59	43	84	145	48	136	682	153	1853	1666	10.1	143	-0.1
52	ZJ-5	2012/06/23	7.74	286	25.7	2760	1	45	123	94	90	34	62	1452	212	3423	3116	9.0	258	0.3
53	ZJ-6	2012/06/23	8.01	295	25.5	2775	0	61	125	148	57	24	67	1524	220	3578	3258	9.0	266	0.6
54	ZJ-7	2012/06/24	7.9	288	24.5	3030	2	76	262	482	80	28	79	1996	291	4681	4335	7.4	345	0.6
55	ZJ-8	2012/06/24	7.99	337	25.2	3030	1	70	189	265	65	25	69	1783	241	4142	3819	7.8	308	0.7
56	ZJ-9	2012/06/24	8.14	375	26.6	3480	2	217	226	163	71	54	89	1832	445	4698	4250	9.5	342	0.9
57	ZJ-10	2012/06/24	7.68	215	27.2	1950	1	65	97	88	114	51	87	1045	164	2555	2289	10.4	192	0.0
60	ZJ-11	2012/06/24	8.02	345	25.2	2943	0	97	202	302	66	31	68	1794	269	4225	3847	9.0	310	0.7
61	ZJ-12	2012/06/25	7.80	260	24.9	2175	2	137	170	148	98	50	102	1267	196	3078	2781	9.7	228	0.2
62	ZJ-13	2012/06/26	7.89	297	27.6	2415	3	153	217	209	87	52	98	1485	215	3549	3205	9.7	260	0.4
64	ZJ-14	2012/06/26	7.84	303	27.8	2505	1	140	211	228	87	47	101	1546	212	3664	3312	9.6	269	0.4
<i>Youjiang River</i>																				
9	YJ-1	2012/06/15	7.96	212	27.2	1750	3	116	103	92	178	53	206	833	183	2290	2156	5.9	181	0.1
10	YJ-2	2012/06/15	7.74	296	25.7	2330	6	131	104	195	107	51	205	1099	226	2907	2960	-1.8	235	0.1
11	YJ-3	2012/06/15	8.04	348	26.6	3290	2	59	130	144	82	30	115	1727	127	3853	3768	2.2	306	0.8
12	YJ-4	2012/06/15	8.07	349	26.4	3260	1	70	169	113	112	28	83	1765	86	3813	3728	2.2	305	0.8
13	YJ-5	2012/06/15	7.8	311	25.7	2720	4	115	111	162	92	43	191	1380	207	3408	3274	3.9	264	0.3
14	YJ-6	2012/06/15	8.09	384	26.0	3620	5	97	247	123	87	35	76	1899	213	4335	4214	2.8	341	0.9
15	YJ-7	2012/06/15	7.92	336	25.9	3070	3	102	121	168	91	36	193	1531	232	3754	3631	3.3	293	0.6
16	YJ-8	2012/06/16	7.67	280	29.3	2380	4	183	155	90	106	61	179	1232	172	3049	2903	4.8	236	0.2
17	YJ-9	2012/06/16	7.67	258	29.5	2270	6	122	131	82	92	36	97	1147	207	2843	2693	5.3	219	0.1
18	YJ-10	2012/06/16	7.68	335	26.8	3050	3	107	130	163	83	37	187	1523	228	3725	3615	2.9	291	0.3
65	YJ-11	2012/06/26	7.86	286	24.8	2595	1	80	84	171	81	38	159	1383	268	3500	3104	11.3	255	0.4
66	YJ-12	2012/06/26	7.78	236	23.7	2295	1	42	90	93	84	22	79	1315	79	2889	2613	9.5	218	0.2
67	YJ-13	2012/06/27	8.23	240	25.1	2070	1	110	69	181	79	50	182	1051	291	2915	2611	10.4	212	0.5
68	YJ-14	2012/06/27	7.85	279	24.7	2610	1	82	72	161	81	38	160	1353	282	3469	3086	11.0	253	0.4
69	YJ-15	2012/06/27	8.46	237	24.9	1965	2	197	14	204	84	50	468	903	291	2907	2586	11.1	208	0.7
70	YJ-16	2012/06/27	8.21	288	24.9	2590	2	112	132	190	111	50	183	1365	282	3526	3216	8.8	263	0.7
71	YJ-17	2012/06/27	7.96	251	24.9	2308	2	146	68	149	183	44	336	1072	279	3082	2821	8.5	235	0.3
72	YJ-18	2012/06/28	8.32	278	27.0	2478	2	130	87	201	155	52	272	1262	263	3375	3099	8.2	255	0.8
73	YJ-19	2012/06/28	8.30	255	25.0	2391	0	61	117	156	118	34	144	1212	232	3066	2881	6.0	236	0.7

Table 1 (continued)

Sample number	Rivers	Date	pH	EC	T	HCO ₃ ⁻	F ⁻	Cl ⁻	NO ₃ ⁻	SO ₄ ²⁻	SiO ₂	K ⁺	Na ⁺	Ca ²⁺	Mg ²⁺	TZ ⁺	TZ ⁻	NICB ^a	TDS	SiC
			(y/m/d)	μS/cm	°C	μmol/l											μeq		%	mg/l
74	YJ-20	2012/06/28	8.10	299	25.0	2724	2	132	196	241	112	60	198	1441	272	3684	3537	4.0	284	0.6
75	YJ-21	2012/06/28	8.24	361	25.9	3405	2	125	154	324	176	54	393	1661	407	4584	4333	5.5	351	0.9
Qingshuihe River																				
45	QS-1	2012/06/21	7.90	283	28.6	2360	5	215	167	152	86	61	114	1340	206	3267	3051	7.0	245	0.4

^a NICB = normalized inorganic charge balance = (TZ⁺ - TZ⁻)/TZ⁺ × 100%.

inputs to rivers (Stallard and Edmond, 1981; Négrel et al., 1993; Gaillardet et al., 1997; Roy et al., 1999). To determine the atmospheric inputs of Cl⁻ to the river waters, the annual mean Cl⁻ concentration of rainwaters collected in the river basins can be multiplied by the evapotranspiration factor. Unfortunately, we have not carried out a systematic study on the chemistry of rainwater in this region. Han et al. (2010b) reported the chemical compositions of rainwaters at Maolan, located near the river basins in Guangxi (Fig. 1). Maolan region is characterized by dense virgin evergreen forests growing on peak cluster karst mountains. This region covers approximately 200 km², underlain by mostly carbonate rock and with forest coverage more than 90% (Han et al., 2010b). The chemical composition of rainwaters in Maolan can provide representative background data of atmospheric deposition. Therefore, the atmospheric inputs calculated here may represent the minimum contributions to the solutes of the river waters.

The volume-weighted mean concentration of Cl⁻ in the rainwaters of Maolan was 5.2 μmol/l (Han et al., 2010b). The mean annual precipitation and evaporation of Guangxi is about 1800 mm and 900 mm, respectively, so an evapotranspiration factor of 2 is applied (Chen et al., 2008). Therefore, it is estimated that about 10.4 μmol/l Cl⁻ is divided from atmosphere. To estimate atmospheric input of the major ions, we make corrections based on the chloride-normalized ratios of the ions in the rainwaters. The Cl-normalized ratios of the rainwaters at Maolan fluctuated widely but most of them were in a relative narrow range. Based on the data reported by Han et al. (2010b), the K⁺/Cl⁻, Na⁺/Cl⁻, Ca²⁺/Cl⁻ and Mg²⁺/Cl⁻ ratios of the rainwaters are calculated to be 0.69 ± 0.35, 0.46 ± 0.24, 2.03 ± 1.14 and 0.30 ± 0.16, respectively. Accordingly, it is estimated that the contribution from the atmosphere to river waters is minor for Na⁺, Ca²⁺, Mg²⁺ (lower than 5%) and only significant for K⁺ (averaging at 21.9 ± 11.1%).

5.1.2. Anthropogenic inputs

Considering the high population density of the Guangxi province, the impact of human activities on water chemistry may be important.

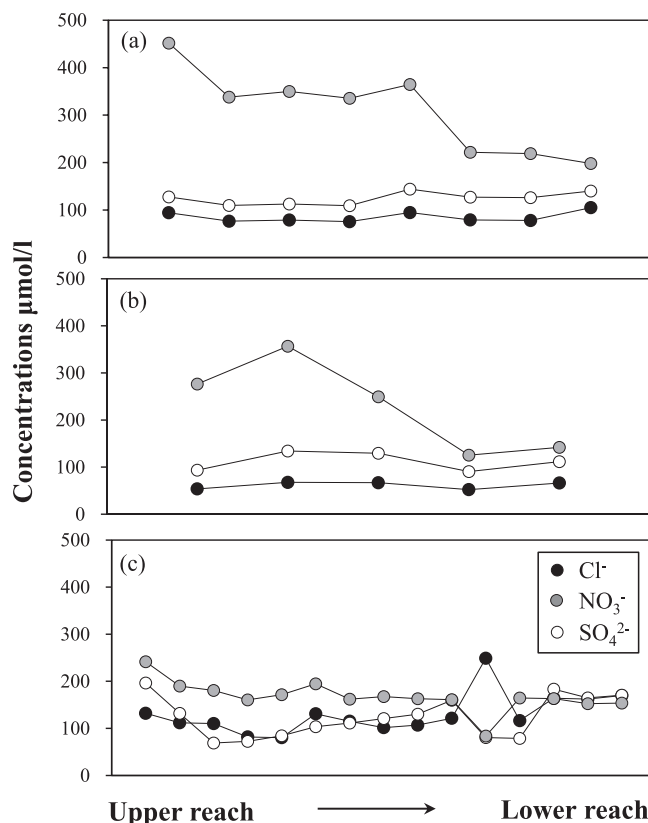


Fig. 3. Evolution of the concentrations of Cl⁻, NO₃⁻ and SO₄²⁻ measured along the mainstream of the Xijiang river (a), the Liujiang river (b) and the Yujiang river (c).

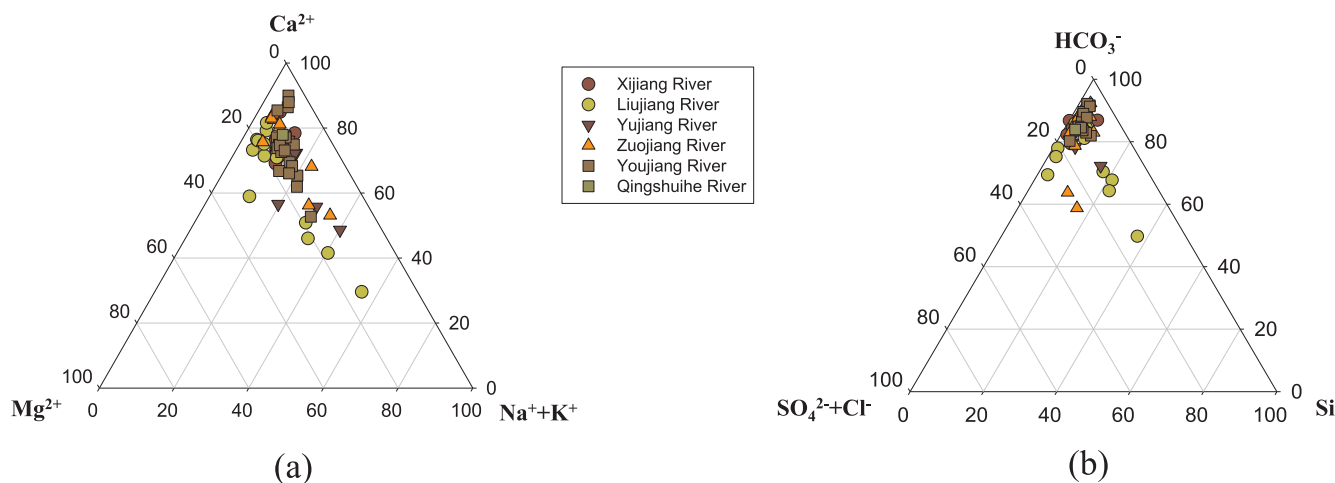


Fig. 2. Ternary diagrams showing cation and anion compositions of the river waters in Guangxi.

Significant changes in Cl^- , NO_3^- and SO_4^{2-} concentrations are observed from the upper reaches to the lower reaches of the mainstream of the Xijiang river, the Liujiang river and the Yujiang river (Fig. 3a–c). Concentrations of Cl^- do not decline with increasing distance from the sea, but have higher concentrations farther inland, which suggests other sources of Cl^- dominate rather than sea-salts (Xu and Liu, 2007; Zhang et al., 2007). The waters have high $\text{NO}_3^-/\text{Na}^+$ molar ratios (average of 1.06), much higher than most of the global rivers (Gaillardet et al., 1999). Meanwhile, Cl^- shares the same variation trend with NO_3^- (Fig. 3) implying the common sources of them, such as fertilizer and sewage (Grosbois et al., 2000). In addition, salt-bearing stratum has not been recorded in Guangxi (Geological Bureau of Guangxi Zhuang Autonomous Region, 1985). Therefore, the excess Cl^- corrected for atmospheric inputs could be ascribed to human activities and balanced by Na^+ . Accordingly, it is estimated that $62.2 \pm 24.0\%$ of the riverine Na^+ is from anthropogenic inputs in average. Anthropogenic inputs of K^+ , Ca^{2+} and Mg^{2+} are not considered in this study (Flintrop et al., 1996; Roy et al., 1999; Liu et al., 2016).

The river waters are also rich in SO_4^{2-} , with high $\text{SO}_4^{2-}/\text{Na}^+$ ratios (averaging at 1.88). However, SO_4^{2-} concentrations do not follow the trends of Cl^- and NO_3^- (Fig. 3a–c), indicating alternative sources of SO_4^{2-} . The riverine SO_4^{2-} may originate from various sources, such as dissolution of gypsum, oxidation of sulfides and acid deposition. It is important to distinguish between these sources because the latter two can produce protons and induce chemical weathering (Amiotte-Suchet et al., 1995; Hercod et al., 1998; Li et al., 2008; Torres et al., 2014, 2016). Guangxi has been a seriously acid deposition affected region for many years. Cheng et al. (2010) reported the average pH of the rainwaters at Liuzhou, Hechi and Wuzhou in Guangxi province was lower than 4.5. Most of the acid rains in the region were SO_4^{2-} -type due to intensive use of S-rich coal (Larsen et al., 1999; Aas et al., 2007). Therefore, acid deposition could have a significant influence on water chemistry in this region. Applying the Cl-normalized ratios of SO_4^{2-} in the rainwaters of Maolan (3.90 ± 2.00 , Han et al., 2010b), it is estimated that approximately $40.6 \pm 20.7 \mu\text{mol/l}$ of the riverine SO_4^{2-} is from acid precipitation. The value is in accordance with the S deposition flux of about 3.1×10^5 to $3.8 \times 10^5 \text{ t/y}$ in Guangxi (Wang et al., 2000; Xu et al., 2006), which could contribute $45.6\text{--}55.9 \mu\text{mol/l}$ SO_4^{2-} to the river waters considering a runoff of about 900 mm (Chen et al., 2008).

Scattered distribution of gypsum mineral deposits within the Xijiang river basin was reported before, and part of the riverine SO_4^{2-} could originate from the dissolution of gypsum (Xu and Liu, 2007; Zhang et al., 2007; Gao et al., 2009). Considering the gypsum-bearing stratum is mainly distributed in the upper reaches of the Xijiang river (mainly in the Nanpanjiang and Beipanjiang river basins) (Zhang et al., 2007; Xu and Liu, 2010), the gypsum contribution should be significant for the mainstream of the Xijiang river. Previous studies reported the riverine SO_4^{2-} from the dissolution of gypsum in the Xijiang river at Wuzhou was about $58.8 \mu\text{mol/l}$ (Chen and He, 1999; Gao et al., 2009). We adopted this value to calculate the contribution of gypsum dissolution to the riverine SO_4^{2-} for the mainstream of the Xijiang river in Guangxi. However, few gypsum mineral deposits and no salt-bearing stratum were recorded in Guangxi (Geological Bureau of Guangxi Zhuang Autonomous Region, 1985), the SO_4^{2-} from the dissolution of gypsum in other rivers is ignored in this work. The other source of SO_4^{2-} in rivers is oxidation of sulfides since coal-bearing sedimentary rocks are widely distributed in the studied region. The SO_4^{2-} concentration from the sulfide oxidation in the river waters is estimated by deducting the SO_4^{2-} from acid precipitation and gypsum dissolution from the total dissolved SO_4^{2-} . Accordingly, $67 \pm 16\%$ of the riverine SO_4^{2-} is from sulfide oxidation in average.

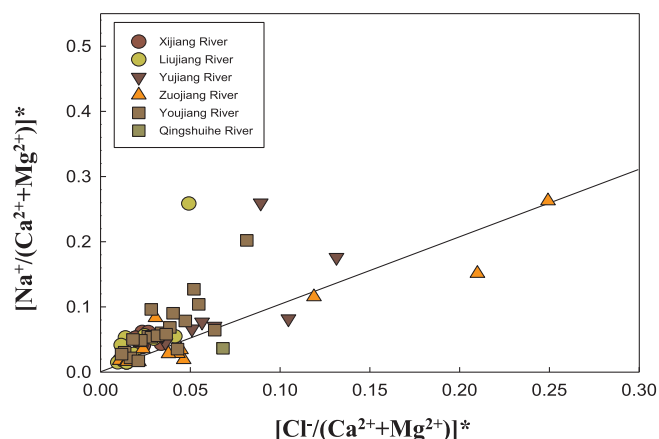


Fig. 4. $[\text{Na}^+ / (\text{Ca}^{2+} + \text{Mg}^{2+})]^*$ plotted against $[\text{Cl}^- / (\text{Ca}^{2+} + \text{Mg}^{2+})]^*$ (equivalent ratio) for the river waters in Guangxi. * Means the value is corrected for atmospheric contribution.

5.1.3. Chemical weathering inputs

In Fig. 4 most of the samples deviate from the 1:1 line, showing a Na^+ excess. This excess Na^+ is attributed to the chemical weathering of silicate. The relationships between $\text{Ca}^{2+}/\text{Na}^+$ and $\text{Mg}^{2+}/\text{Na}^+$, $\text{Ca}^{2+}/\text{Na}^+$ and $\text{HCO}_3^-/\text{Na}^+$ molar ratios are presented in Fig. 5. Good correlations are observed between $(\text{Ca}^{2+}/\text{Na}^+)^*$ and $(\text{Mg}^{2+}/\text{Na}^+)^*$ ($R^2 = 0.85$, $n = 68$), and between $(\text{Ca}^{2+}/\text{Na}^+)^*$ and $(\text{HCO}_3^-/\text{Na}^+)^*$ ($R^2 = 0.99$, $n = 68$). They would appear to indicate different mixing trends in rivers of at least two end-members, carbonate and silicate weathering. Rivers draining carbonate regions have high $\text{Mg}^{2+}/\text{Na}^+$, $\text{Ca}^{2+}/\text{Na}^+$ and $\text{HCO}_3^-/\text{Na}^+$ ratios of approximately 5–10, 10–50 and 20–80, respectively, which are consistent with the values for carbonate end-member estimated by Gaillardet et al. (1999). According to the lithological background (Fig. 1), dolomitic limestone and dolomite are widely distributed in Guangxi. The covariation of $\text{Mg}^{2+}/\text{Ca}^{2+}$ and $\text{Na}^+/\text{Ca}^{2+}$ molar ratios shows that three end-members are recognizable, which are limestone, dolomite and silicate weathering (Fig. 6). The dolomite end-member is characterized by high $\text{Mg}^{2+}/\text{Ca}^{2+}$ ratio of about 1.1 and low $\text{Na}^+/\text{Ca}^{2+}$ ratio of about 0.02, while the limestone end-member has low $\text{Mg}^{2+}/\text{Ca}^{2+}$ and $\text{Na}^+/\text{Ca}^{2+}$ ratios of 0.1 and 0.02, respectively (Han and Liu, 2004).

After correction of the precipitation and anthropogenic inputs, all the remaining Na^+ and K^+ are assumed to derive from silicate weathering. Ca^{2+} and Mg^{2+} deriving from silicate weathering can be calculated using the $\text{Ca}^{2+}/\text{Na}^+$ and $\text{Mg}^{2+}/\text{Na}^+$ molar ratios of silicate end-member. In this study, the $\text{Ca}^{2+}/\text{Na}^+$ ratio of 0.4 and $\text{Mg}^{2+}/\text{Na}^+$ ratio of 0.2 are adopted according to the estimations by Zhang et al. (2007). They compiled the $\text{Ca}^{2+}/\text{Na}^+$ and $\text{Mg}^{2+}/\text{Na}^+$ ratios based on rivers draining silicate lithology in the Pearl river (Zhujiang) basin. Previous studies reported the $\text{Ca}^{2+}/\text{Na}^+$ and $\text{Mg}^{2+}/\text{Na}^+$ ratios of silicate end-member in global river basins. Wu et al. (2008) applied the $(\text{Ca}/\text{Na})_{\text{sil}}$ ratio of 0.17–0.58 in the study of seven rivers that originate in the Tibetan Plateau. Wang et al. (2016) applied the $(\text{Ca}/\text{Na})_{\text{sil}}$ values of 0.25–0.31 for the Huanghe (Yellow) river. Galy and France-Lanord (1999) applied $(\text{Ca}/\text{Na})_{\text{sil}}$ values of 0.15–0.25, and Krishnaswami et al. (1999) applied $(\text{Ca}/\text{Na})_{\text{sil}}$ and $(\text{Mg}/\text{Na})_{\text{sil}}$ values of 0.7 ± 0.3 and 0.3 ± 0.2 , respectively, for the Ganges-Brahmaputra basin. In the world's large rivers, $\text{Ca}/\text{Na} = 0.35 \pm 0.15$ and $\text{Mg}/\text{Na} = 0.24 \pm 0.12$ were assigned to the silicate end-member by Gaillardet et al. (1999). An uncertainty of 50% for $\text{Ca}^{2+}/\text{Na}^+$ and $\text{Mg}^{2+}/\text{Na}^+$ of silicate end-member is considered in this study as other authors did. It is estimated that $33.6 \pm 1.6\%$ of Na^+ , $78.1 \pm 11.1\%$ of K^+ , $3.3 \pm 1.7\%$ of Ca^{2+} and

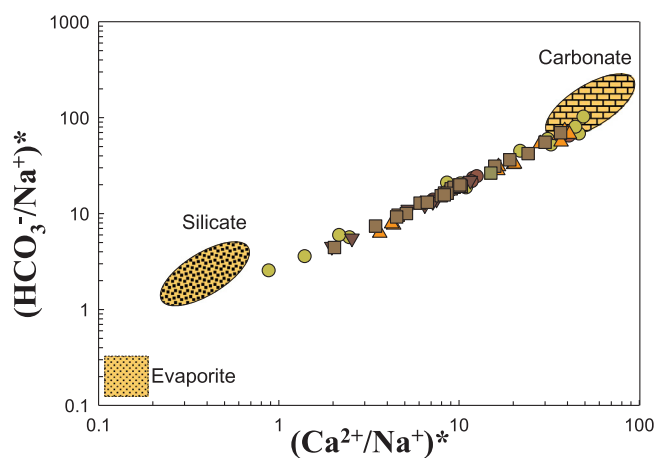
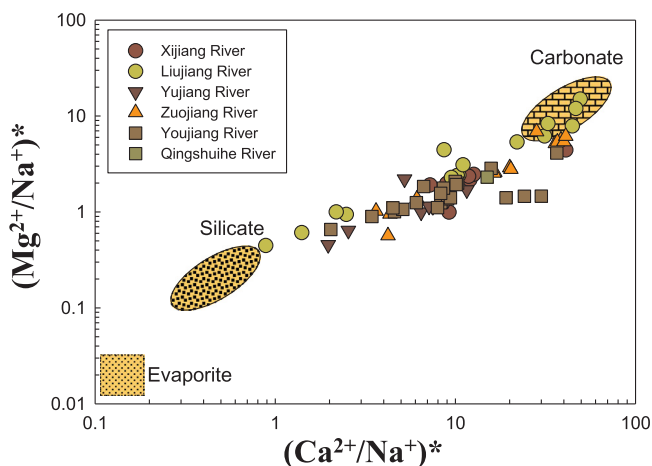


Fig. 5. Correlations between $(Mg^{2+}/Na^+)^*$, $(HCO_3^-/Na^+)^*$ and $(Ca^{2+}/Na^+)^*$ (molar ratio) of the river waters in Guangxi, showing mixing between silicate and carbonate end-members. The silicate, carbonate and evaporite endmembers are from Gaillardet et al. (1999). * Means the value is corrected for atmospheric and anthropogenic contribution.

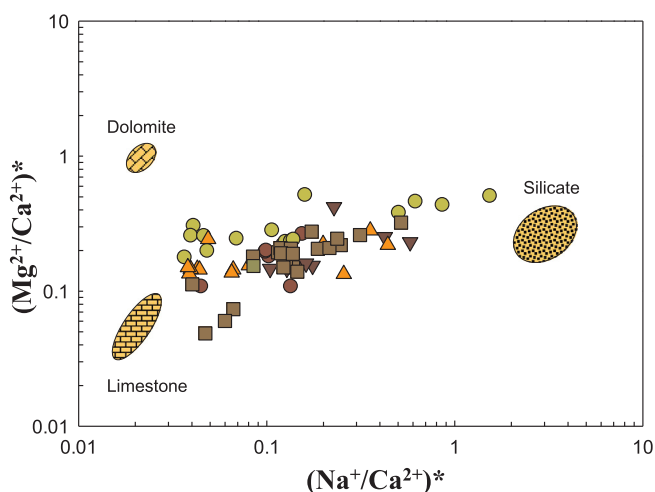


Fig. 6. Correlations between $(Na^+/Ca^{2+})^*$ and $(Mg^{2+}/Ca^{2+})^*$ (molar ratio) of the river waters in Guangxi, showing mixing between silicate, dolomite and limestone end-members. End-members are from Han and Liu, 2004. * Means the value is corrected for atmospheric and anthropogenic contribution.

$6.2 \pm 3.1\%$ of Mg^{2+} in the river waters are from silicate weathering. The estimation of Ca^{2+} and Mg^{2+} from carbonate weathering is made by deducting the atmospheric and silicate contributions from the total Ca^{2+} and Mg^{2+} concentrations.

5.2. Contributions of the sources

In the following discussions, we attempt to quantify the contribution of the different sources of the solutes to the river waters by a straight forward method (Galy and France-Lanord, 1999). Chemical composition of river water is controlled by atmospheric, anthropogenic inputs, evaporite dissolution and chemical weathering of silicate and carbonate. The mass budget equation for any element X in the dissolved load (in molar concentration) can be written as:

$$[X]_{riv} = [X]_{atm} + [X]_{anth} + [X]_{evap} + [X]_{sil} + [X]_{carb} \quad (3)$$

The calculation is based on some straightforward simplifications as we discussed in Section 5.1. The calculated contributions of different sources to the total cationic loads for the rivers draining Guangxi are

illustrated in Fig. 7. The results show that the contributions of different reservoirs are 1.8–3.2% for atmospheric input, 2.6–6.5% for anthropogenic input, 2.6–10.2% for silicate weathering and 84.9–92.5% for carbonate weathering, respectively. The evaporite dissolution contributes 12.4% and 4.0% of the cationic loads in the mainstream of the Xijiang river at Tian'e and Wuzhou, respectively. The cationic loads of the rivers are dominated by carbonate weathering. The highest anthropogenic contributions are observed for the samples from the most developed regions of Guangxi (e.g. sample 20 at Nanning). The high silicate contributions are observed for the rivers draining metamorphic and igneous regions (e.g. samples 24, 35, 36 and 37). The proportions of the cations from limestone and dolomite are also calculated. The result shows that about 81% of the cations deriving from carbonate weathering is from limestone.

5.3. Chemical weathering and CO_2 consumption rates

The sulfuric acid derived from the oxidation of sulfide and acid precipitation might be involved in both silicate and carbonate weathering reactions. It is assumed that silicate and carbonate weathering by sulfuric acid occur in the same ratio as those by carbonic acid (Galy and France-Lanord, 1999; Spence and Telmer, 2005; Liu et al., 2016). The mass balance equations can be written as:

$$[SO_4^{2-}]_{CW} = [SO_4^{2-}]_{river} - [SO_4^{2-}]_{evaporite} = [SO_4^{2-}]_{SCW} + [SO_4^{2-}]_{SSW} \quad (4)$$

$$[SO_4^{2-}]_{SCW} = [SO_4^{2-}]_{CW}/(A + 1) \quad (5)$$

where $[SO_4^{2-}]_{CW}$, $[SO_4^{2-}]_{SCW}$ and $[SO_4^{2-}]_{SSW}$ represent sulfuric acid consumed by chemical weathering, the fractions of sulfuric acid consumed by carbonate weathering and the fractions of sulfuric acid consumed by silicate weathering, respectively. A is the ratio of carbonic acid consumed by silicate weathering to carbonic acid consumed by carbonate weathering.

Bicarbonate resulting from the weathering of carbonates by sulfuric acid ($[HCO_3^-]_{SCW}$) and carbonic acid ($[HCO_3^-]_{CCW}$) is calculated as:

$$[HCO_3^-]_{SCW} = 2[SO_4^{2-}]_{SCW} = 2[Ca^{2+} + Mg^{2+}]_{SCW} \quad (6)$$

$$[HCO_3^-]_{CCW} = 2[Ca^{2+} + Mg^{2+}]_{CCW} \quad (7)$$

Bicarbonate resulting from the weathering of silicates by carbonic acid ($[HCO_3^-]_{CSW}$) is calculated as:

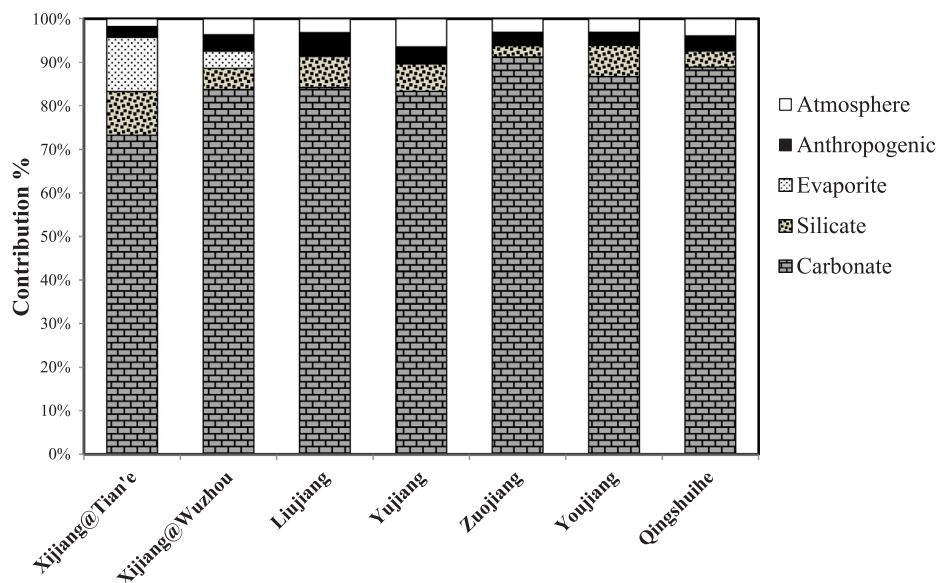


Fig. 7. Calculated contributions of different reservoirs to the cationic loads (in mg/l) for the rivers in Guangxi.

$$[\text{HCO}_3^-]_{\text{CSW}} = [\text{Na}^+ + \text{K}^+]_{\text{CSW}} + 2[\text{Ca}^{2+} + \text{Mg}^{2+}]_{\text{CSW}} \quad (8)$$

The chemical weathering rate of rocks is estimated by the mass budget and the surface area and water discharges of the river basins. The carbonate weathering rate (CWR) is calculated using the concentrations of Ca^{2+} , Mg^{2+} and HCO_3^- produced by carbonate weathering by both sulfuric and carbonic acid.

$$\text{CWR} = (\text{Ca}_{\text{carb}}^{2+} + \text{Mg}_{\text{carb}}^{2+} + [\text{HCO}_3^-]_{\text{SCW}} + 0.5[\text{HCO}_3^-]_{\text{CCW}}) \times \text{discharge/area} \quad (9)$$

The silicate weathering rate (SWR) is calculated using the concentrations of Na^+ , K^+ , Ca^{2+} , Mg^{2+} and SiO_2 produced by silicate weathering. It is assumed that all of the dissolved SiO_2 in the river water is from silicate weathering (Gaillardet et al., 1999).

$$\text{SWR} = (\text{Na}_{\text{sil}}^+ + \text{K}_{\text{sil}}^+ + \text{Ca}_{\text{sil}}^{2+} + \text{Mg}_{\text{sil}}^{2+} + \text{SiO}_2) \times \text{discharge/area} \quad (10)$$

The CO_2 consumption by silicate weathering ($\text{CO}_{2\text{sil}}$) and carbonate weathering ($\text{CO}_{2\text{carb}}$) can be calculated based on the charge balance after different weathering agents are assessed:

$$\text{CO}_{2\text{carb}} = (2[\text{Ca}^{2+} + \text{Mg}^{2+}]_{\text{carb}} - [\text{HCO}_3^-]_{\text{SCW}})/2 \quad (11)$$

$$\text{CO}_{2\text{sil}} = \text{Na}_{\text{sil}}^+ + \text{K}_{\text{sil}}^+ + 2\text{Ca}_{\text{sil}}^{2+} + 2\text{Mg}_{\text{sil}}^{2+} - 2[\text{SO}_4^{2-}]_{\text{SSW}} \quad (12)$$

Samples 3, 28, 26, 27, 64, 18 and 45 are used to calculate the rock weathering and CO_2 consumption rates of the Xijiang river basin (at Tian'e), the Xijiang river basin (at Wuzhou), the Liujiang river basin, the Yujiang river basin, the Zuojiang river basin, the Youjiang river basin and the Qingshuihe river basin, respectively. The results of chemical weathering and CO_2 consumption rates for these river basins are listed in Table 2. The silicate weathering rates range from 2.9 t/km²/yr for the Qingshuihe river basin to 7.9 t/km²/yr for the Liujiang river basin. The carbonate weathering rates range from 61.4 t/km²/yr for the Qingshuihe river basin to 93.3 t/km²/yr for the Zuojiang river basin. For the Xijiang river basin, the silicate/carbonate weathering rates at Tian'e and Wuzhou are 5.6/76.6 t/km²/yr and 5.1/89.4 t/km²/yr, respectively. Sulfuric acid-induced chemical weathering accounts for about 10.0%, 14.5%, 11.8%, 13.1%, 9.2% and 9.8% of the total weathering rates of the Xijiang (at Wuzhou), the Liujiang, the Yujiang, the Zuojiang, the Youjiang and the Qingshuihe river basins, respectively.

The CO_2 consumption rates by silicate weathering range from 19×10^3 mol/km²/yr for the Zuojiang river basin to 85×10^3 mol/km²/yr for the Liujiang river basin. The CO_2 consumption rates by carbonate weathering range from 559×10^3 mol/km²/yr for the Qingshuihe river basin to 817×10^3 mol/km²/yr for the Zuojiang river basin. The CO_2 consumption rates by silicate and carbonate weathering for the Xijiang river basin at Wuzhou are 58×10^3 and 816×10^3 mol/km²/yr, respectively. The CO_2 consumption rates are 85–91% of the value calculated with the assumption that carbonic acid serves as the only weathering agent. The total chemical weathering and CO_2 consumption rates of the river basins in Guangxi can be calculated by deducting the fluxes of the upper reaches of Guangxi (sample 3 at Tian'e) from the fluxes of the downstream sampling site (sample 28 at Wuzhou). The total chemical weathering rates of silicate and carbonate by carbonic/sulfuric acid of the river basins in Guangxi are 5.1/0.5 t/km²/yr and 97.8/9.6 t/km²/yr, respectively. The total chemical weathering rate is 112.9 t/km²/yr, which is higher than the upper reaches of the Xijiang river (the Nanpanjiang and Beipanjiang river basins) on the Yunnan-Guizhou Plateau. This may be attributed to higher precipitation, temperature and more developed karstic landforms in Guangxi than the upper reaches (Xu and Liu, 2007; Gao et al., 2009). As highlighted by many researchers (e.g. White and Blum, 1995; Gaillardet et al., 1999; Millot et al., 2003; Oliva et al., 2003), runoff and temperature are important factors controlling chemical weathering rate. The total CO_2 consumption rates by carbonate and silicate weathering of the river basins in Guangxi are 987×10^3 mol/km²/yr and 18×10^3 mol/km²/yr, respectively, which account for 1.6% and 0.1% of the global CO_2 consumption fluxes (12.3×10^{12} and 8.7×10^{12} mol/yr, Gaillardet et al., 1999), respectively. Considering the chemical weathering flux (3.0×10^7 t/yr) and CO_2 consumption flux (338×10^9 mol/yr) of the whole Xijiang river basin reported by Xu and Liu (2010), about 75% of the chemical weathering flux and 60% of the CO_2 consumption flux of the Xijiang river basin occur in Guangxi.

5.4. Disturbances of sulfuric acid to the CO_2 budget

The carbon budget of chemical weathering is dependent on the CO_2 release from sulfuric acid-driven carbonate weathering and the CO_2 consumption by silicate and/or carbonate weathering. The short- and

Table 2
Chemical weathering and CO₂ consumption rates of the river basins in Guangxi.

River basins	Location	Discharge (10 ⁸ m ³ /yr)	Surface area (km ²)	Rock weathering rate		Total weathering rate				CO ₂ consumption rate-silicates		CO ₂ consumption rate-carbonates		
				Carbonic acid	Sulfuric acid	Carbonates (t/km ² /yr)	Sulfuric acid	Total	Carbonic acid	Sulfuric acid	Total	10 ⁹ mol/yr	10 ³ mol/km ² /yr	10 ⁹ mol/yr
Xijiang	Tiane	510	98,500	4.9 ± 0.6	0.72 ± 0.2	5.6 ± 0.8	66.7 ± 2.0	9.9 ± 0.6	76.6 ± 2.6	83.2 ± 3.0	15.1 ± 3.6	153 ± 31	67.5 ± 2.0	685 ± 18
Xijiang	Wuzhou	2200	327,000	4.6 ± 0.3	0.5 ± 0.1	5.1 ± 0.4	80.5 ± 1.1	8.9 ± 0.2	89.4 ± 1.3	94.5 ± 1.7	18.8 ± 5.2	58 ± 15	266.9 ± 3.8	816 ± 12
Liujiang	Liuzhou	527	58,270	6.7 ± 0.5	1.1 ± 0.1	7.9 ± 0.6	71.5 ± 1.8	12.2 ± 0.3	83.7 ± 2.1	91.6 ± 2.7	5.0 ± 1.4	85 ± 23	42.5 ± 1.1	728 ± 19
Yujiang	Guiping	502	89,870	4.2 ± 0.2	0.6 ± 0.1	4.8 ± 0.3	61.8 ± 1.0	8.3 ± 0.1	70.1 ± 1.0	74.9 ± 1.3	4.5 ± 0.8	50 ± 10	56.1 ± 0.8	624 ± 9
Zuojiang	Songcun	174	32,068	3.2 ± 0.1	0.5 ± 0.02	3.7 ± 0.1	84.1 ± 1.0	12.3 ± 0.1	93.3 ± 1.0	97.0 ± 1.1	0.6 ± 0.06	19 ± 2	26.2 ± 0.2	817 ± 7
Youjiang	Songcun	145	38,612	3.4 ± 0.4	0.3 ± 0.1	3.7 ± 0.5	56.6 ± 1.5	5.8 ± 0.2	62.3 ± 1.6	66.1 ± 2.1	2.7 ± 0.9	74 ± 25	22.1 ± 0.6	571 ± 15
Qingshuhe	Zouxu	17	4,169	2.7 ± 0.1	0.3 ± 0.01	2.9 ± 0.1	55.3 ± 0.4	6.1 ± 0.1	61.4 ± 0.5	64.4 ± 0.6	0.1 ± 0.01	20 ± 1	2.3 ± 0.02	559 ± 4
Xijiang river basin in Guangxi		1690	202,000	5.1 ± 0.2	0.5 ± 0.1	5.6 ± 0.3	97.8 ± 0.8	9.6 ± 0.1	107.4 ± 0.9	112.9 ± 1.2	3.7 ± 1.6	18 ± 8	199.4 ± 1.8	987 ± 10

long-term effects of sulfuric acid weathering on atmospheric CO₂ were discussed in previous studies (e.g. [Calmels et al., 2007](#); [Torres et al., 2014](#)). The proportions of weathering driven by sulfuric acid are plotted against the proportions of cations from carbonate weathering to explore the spatial distribution of the effects of chemical weathering on atmospheric CO₂ ([Fig. 8](#)) ([Torres et al., 2016](#)). The grey line and black line are the limits that yield no change in atmospheric CO₂ over 10⁵–10⁶ yrs (shorter than that of carbonate burial) and 10⁷ yrs (longer than that of carbonate burial but shorter than that of pyrite burial) ([Bernier and Bernier, 2012](#)), respectively. The assumptions and establishment of the equations of the limits in [Fig. 8](#) are given in detail in the Appendix A.

The proportions of cation sourced from carbonate weathering show a narrow range, except for some samples collected from metamorphic and igneous regions (e.g. samples 35 and 36 of the Liujiang and 24 of the Yujiang river) ([Fig. 8](#)). The proportions of weathering driven by sulfuric acid range from 5 to 44%, with the high values observed for the rivers in high elevation regions (e.g. 44%, 31% and 35% for the samples 39, 40 and 41 of the Liujiang river basin, respectively) ([Fig. 8](#)). The results are consistent with the expectation that the ratio of sulfide oxidation to weathering increases with increasing elevation ([Torres et al., 2014, 2016](#)).

For most of the sites, high sulfuric acid weathering leads to CO₂ release into the atmosphere, while only a few sites with low proportions of carbonate weathering and/or low proportions of sulfuric acid weathering are acting as carbon sink ([Fig. 8](#)). The major river basins in Guangxi are carbon sources on timescales of 10⁷ yrs (see the insert in [Fig. 8](#)). This is also well documented for the Mackenzie river in Canada, the Liwu river in Taiwan and the Kosñipata river in high Andes ([Calmels et al., 2007, 2011](#); [Das et al., 2012](#); [Torres et al., 2014, 2016](#)). According to [Torres et al. \(2016\)](#), sulfuric acid weathering can lead to CO₂ release into the atmosphere on short timescales (10⁵ to 10⁶ yrs) in Andes mountainous region. The proportions of sulfuric acid weathering of the river basins in Guangxi are not high enough for CO₂ release on short timescales. Therefore, sulfuric acid-induced weathering has great climatic implication on both short and long timescales ([Calmels et al., 2007](#); [Torres et al., 2016](#)).

The effect of the sulfuric acid (sulfide oxidation and acid rain) on the CO₂ budget is estimated. The flux of SO₄²⁻ derived from sulfide oxidation is estimated at 12.6 ± 3.4 × 10⁹ mol/yr based on the difference between the flux of sulfide oxidation-derived SO₄²⁻ in the mainstream of the Xijiang river at Tian'e and Wuzhou. The same amount of CO₂ will be released to the atmosphere, which would exceed the amount of CO₂ consumed by silicate weathering (3.7 ± 1.6 × 10⁹ mol/yr) in the river basins. Therefore, Guangxi region is a net CO₂ source on geological timescales (10⁷ yrs), and the net CO₂ releasing flux is 8.9 ± 5.0 × 10⁹ mol/yr (or 0.11 ± 0.06 × 10¹² gC/yr). Further considering the sulfuric acid derived from acid rain, the long-term net releasing flux of CO₂ is approximately 15.7 ± 5.0 × 10⁹ mol/yr (or 0.19 ± 0.06 × 10¹² g C/yr). This study highlights the fact that CO₂ budget will be largely altered by sulfuric acid, especially in seriously acid deposition affected region.

6. Conclusions

The major ionic compositions of the river waters from the major river basins in Guangxi, South China, are investigated in this study. Carbonate weathering dominates the water chemistry, which contributes 85–93% of the total cationic loads of the river waters. The riverine SO₄²⁻ are mainly derived from acid precipitation and the oxidation of sulfide. The total chemical weathering rates of silicate and carbonate by carbonic/sulfuric acid of the river basins in Guangxi are 5.1/0.5 and 97.8/9.6 t/km²/yr, respectively. The total CO₂ consumption rates by silicate and carbonate weathering are 18 × 10³ and 987 × 10³ mol/km²/yr, respectively. The CO₂ consumption rates are only 85–91% of the value calculated with the assumption that carbonic acid

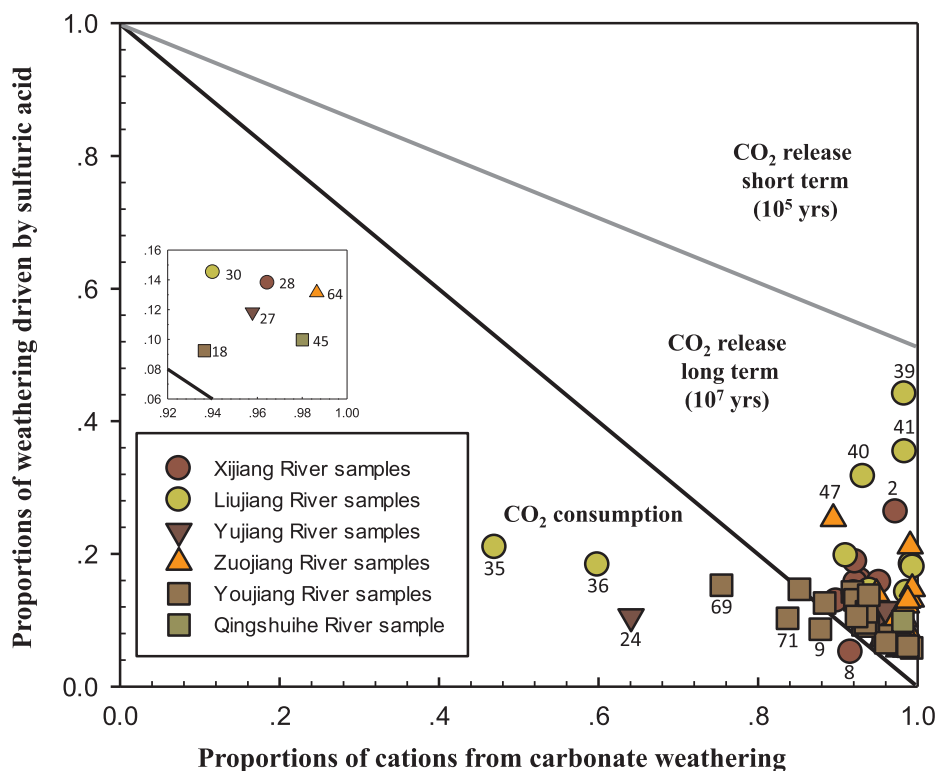


Fig. 8. Diagram showing the effect of chemical weathering on atmospheric CO₂. The long term and short term consequences are considered. Proportions of weathering driven by sulfuric acid is calculated by $SO_4^{2-}/\Sigma_{\text{weathering}}^+$, and proportions of cations from carbonate weathering is calculated by $\Sigma_{\text{carbonate}}^+/\Sigma_{\text{weathering}}^+$ (equivalent ratio). The insert is an expanded view for the major rivers and the mainstream of the Xijiang river (at Wuzhou).

serves as the only weathering agent. The involvement of sulfuric acid in the chemical weathering makes the river basins in Guangxi net CO₂ sources on timescales of 10⁷ yrs, and the total releasing flux is $15.7 \pm 5.0 \times 10^9$ mol/yr (or $0.19 \pm 0.06 \times 10^{12}$ gC/yr). The result highlights the important role of sulfuric acid in chemical weathering in the karst region.

Acknowledgments

We thank the handling editor and the anonymous reviewer for their constructive comments and suggestions. This work was financially supported by National Natural Science Foundation of China (Grant No. 91747202, 41730857, 41173114 and 41673020).

Appendix A. The effect of weathering driven by sulfuric acid on carbon budget over different timescales

The proportions of carbonate weathering and weathering by sulfuric acid can be used to predict the effect of weathering on atmospheric CO₂ (Torres et al., 2016). Proportions of weathering driven by sulfuric acid is calculated by $SO_4^{2-}/\Sigma_{\text{weathering}}^+$, and proportions of cations from carbonate weathering is calculated by $\Sigma_{\text{carbonate}}^+/\Sigma_{\text{weathering}}^+$ (in equivalent ratio). Equations are set in order to solve for parameter combinations that yield no change in atmospheric CO₂ over different timescales in Fig. 8. (Torres et al., 2016). On time scales shorter than that of carbonate burial (10⁵ to 10⁶ yrs; Berner and Berner, 2012), carbonic acid-driven carbonate and silicate weathering consumes atmospheric CO₂, while sulfuric acid-driven carbonate weathering releases CO₂. The equation can be written:

$$0.5\Sigma_{\text{carbonate}}^+ \times z = (\Sigma_{\text{carbonate}}^+ + \Sigma_{\text{silicate}}^+) \times (1 - z) \tag{A1}$$

which gives the relationship:

$$z = 1 - 0.5\Sigma_{\text{carbonate}}^+ / (\Sigma_{\text{carbonate}}^+ + \Sigma_{\text{silicate}}^+) \tag{A2}$$

where z is the proportion of weathering driven by sulfuric acid. In Fig. 8 data that plot above the grey limit described by Eq. (A2) are associated with CO₂ release on timescales shorter than carbonate precipitation.

On time scales longer than that of carbonate burial (10⁵ to 10⁶ yrs) but shorter than that of pyrite burial (10⁷ yrs) (Berner and Berner, 2012), carbonic acid-driven silicate weathering is the only CO₂ sink. The equation can be written:

$$0.5\Sigma_{\text{carbonate}}^+ \times z = 0.5\Sigma_{\text{silicate}}^+ \times (1 - z) \tag{A3}$$

which gives the relationship:

$$z = 1 - \Sigma_{\text{carbonate}}^+ / (\Sigma_{\text{carbonate}}^+ + \Sigma_{\text{silicate}}^+) \tag{A4}$$

In Fig. 8, data that plot above the black limit described by Eq. (A4) are associated with CO₂ release on timescales longer than carbonate precipitation, but shorter than pyrite burial.

References

Aas, W., Shao, M., Jin, L., Larssen, T., Zhao, D., Xiang, R., Zhang, J., Xiao, J., Duan, L.,

2007. Air concentrations and wet deposition of major inorganic ions at five nonurban sites in China, 2001–2003. Atmos. Environ. 41 (8), 1706–1716.
Amiotte-Suchet, P., Probst, A., Probst, J.-L., 1995. Influence of acid rain on CO₂ consumption by rock weathering: local and global scales. Water Air Soil Pollut. 85 (3),

- 1563–1568.
- Berner, R.A., 1991. A model for atmospheric CO₂ over Phanerozoic time. *Am. J. Sci.* 291, 339–376.
- Berner, E.K., Berner, R.A., 2012. *Global Environment: Water, Air, and Geochemical Cycles*. Princeton University Press.
- Berner, R.A., Kothavala, Z., 2001. GEOCARB III: a revised model of atmospheric CO₂ over Phanerozoic time. *Am. J. Sci.* 301 (2), 182–204.
- Berner, R.A., Lasaga, A.C., Garrels, R.M., 1983. The carbonate-silicate geochemical cycle and its effect on atmospheric carbon-dioxide over the past 100 million years. *Am. J. Sci.* 283 (283), 641–683.
- Calmels, D., Gaillardet, J., Brenot, A., France-Lanord, C., 2007. Sustained sulfide oxidation by physical erosion processes in the Mackenzie River basin: climatic perspectives. *Geology* 35 (11), 1003–1006.
- Calmels, D., Galy, A., Hovius, N., Bickle, M., West, A.J., Chen, M.-C., Chapman, H., 2011. Contribution of deep groundwater to the weathering budget in a rapidly eroding mountain belt, Taiwan. *Earth Planet. Sci. Lett.* 303 (1–2), 48–58.
- Chen, B., Pan, J., Liao, S., Lin, K., Huang, L., 2008. Evaporation calculation of in Guangxi and its temporal and spatial distribution characteristics. *J. Meteorol. Res. Appl.* 29 (1), 29–33 (in Chinese, with English Abstr.).
- Chen, J.S., He, D.W., 1999. Chemical characteristics and genesis of major ions in the Pearl River Basin. *Acta Sci. Nat. Univ. Pekinensi* 35, 786–793 (in Chinese, with English Abstr.).
- Cheng, A.Z., Wei, H.H., Tan, F., 2010. Analysis of the temporal-spatial distribution and seasonal variation of the acid rain in Guangxi Province. *Meteorol. Environ. Res.* 1 (1), 62–65.
- Chetelat, B., Liu, C.-Q., Zhao, Z.-Q., Wang, Q.-L., Li, S.-L., Li, J., Wang, B.-L., 2008. Geochemistry of the dissolved load of the Changjiang Basin rivers: anthropogenic impacts and chemical weathering. *Geochim. Cosmochim. Acta* 72 (11), 4254–4277.
- Das, A., Chung, C.H., You, C.F., 2012. Disproportionately high rates of sulfide oxidation from mountainous river basins of Taiwan orogeny: sulfur isotope evidence. *Geophys. Res. Lett.* 39 (12), 1–6.
- Flintrop, C., Hohlmann, B., Jasper, T., Korte, C., Podlaha, O.G., Scheele, S., Veizer, J., 1996. Anatomy of pollution; rivers of North Rhine-Westphalia, Germany. *Am. J. Sci.* 296 (1), 58–98.
- Gaillardet, J., Dupre, B., Allègre, C.J., Nègre, P., 1997. Chemical and physical denudation in the Amazon River basin. *Chem. Geol.* 142 (3–4), 141–173.
- Gaillardet, J., Dupré, B., Louvat, P., Allègre, C.J., 1999. Global silicate weathering and CO₂ consumption rates deduced from the chemistry of large rivers. *Chem. Geol.* 159 (1–4), 3–30.
- Gaillardet, J., Galy, A., 2008. Himalaya: carbon sink or source? *Science* 320 (5884), 1727–1728.
- Galy, A., France-Lanord, C., 1999. Weathering processes in the Ganges-Brahmaputra basin and the riverine alkalinity budget. *Chem. Geol.* 159 (1–4), 31–60.
- Gao, Q., Tao, Z., Huang, X., Nan, L., Yu, K., Wang, Z., 2009. Chemical weathering and CO₂ consumption in the Xijiang River basin, South China. *Geomorphology* 106 (3), 324–332.
- Geological Bureau of Guangxi Zhuang Autonomous Region, 1985. *Regional Geological Archive of Guangxi Zhuang Autonomous Region*. Geological Publishing House, Beijing, China (in Chinese).
- Grosbois, C., Nègre, P., Fouillat, C., Grimaud, D., 2000. Dissolved load of the Loire River: chemical and isotopic characterization. *Chem. Geol.* 170 (1–4), 179–201.
- Han, G., Liu, C.-Q., 2004. Water geochemistry controlled by carbonate dissolution: a study of the river waters draining karst-dominated terrain, Guizhou Province, China. *Chem. Geol.* 204 (1), 1–21.
- Han, G., Tang, Y., Xu, Z., 2010a. Fluvial geochemistry of rivers draining karst terrain in Southwest China. *J. Asian Earth Sci.* 38 (1–2), 65–75.
- Han, G., Tang, Y., Wu, Q., Tan, Q., 2010b. Chemical and strontium isotope characterization of rainwater in karst virgin forest, southwest china. *Atmos. Environ.* 44 (2), 174–181.
- Hercod, D.J., Brady, P.V., Gregory, R.T., 1998. Catchment-scale coupling between pyrite oxidation and calcite weathering. *Chem. Geol.* 151 (1), 259–276.
- Kashiwagi, H., Ogawa, Y., Shikazono, N., 2008. Relationship between weathering, mountain uplift, and climate during the Cenozoic as deduced from the global carbon-strontium cycle model. *Palaeogeography* 270 (1), 139–149.
- Krishnaswami, S., Singh, S.K., Dalai, T.K., 1999. Silicate weathering in the Himalaya: role in contributing to major ions and radiogenic Sr to the Bay of Bengal. *Ocean Science, Trends and Future Directions*, 23–51.
- Larssen, T., Seip, H.M., Semb, A., Mulder, J., Muniz, I.P., Vogt, R.D., Lydersen, E., Angell, V., Tang, D., Eilertsen, O., 1999. Acid deposition and its effects in China: an overview. *Environ. Sci. Policy* 2 (1), 9–24.
- Lerman, A., Wu, L., Mackenzie, F.T., 2007. CO₂ and H₂SO₄ consumption in weathering and material transport to the ocean, and their role in the global carbon balance. *Mar. Chem.* 106 (1–2), 326–350.
- Li, S., Zhang, Q., 2008. Geochemistry of the upper han River Basin, China, 1: spatial distribution of major ion compositions and their controlling factors. *Appl. Geochem.* 23 (12), 3535–3544.
- Li, S.-L., Calmels, D., Han, G., Gaillardet, J., Liu, C.-Q., 2008. Sulfuric acid as an agent of carbonate weathering constrained by $\delta^{13}\text{C}_{\text{DIC}}$: examples from Southwest China. *Earth Planet. Sci. Lett.* 270 (3), 189–199.
- Li, S.-L., Chetelat, B., Yue, F., Zhao, Z., Liu, C.-Q., 2014. Chemical weathering processes in the Yalong River draining the Eastern Tibetan Plateau, China. *J. Asian Earth Sci.* 88 (88), 74–84.
- Liu, W.-J., Shi, C., Xu, Z., Zhao, T., Jiang, H., Liang, C., Zhang, X., Zhou, L., Yu, C., 2016. Water geochemistry of the Qiantangjiang River, east China: chemical weathering and CO₂ consumption in a basin affected by severe acid deposition. *J. Asian Earth Sci.* 127, 246–256.
- Millot, R., Gaillardet, J.B.D., Allègre, C.J., 2003. Northern latitude chemical weathering rates: clues from the Mackenzie River basin, Canada. *Geochim. Cosmochim. Acta* 67 (7), 1305–1329.
- Moon, S., Chamberlain, C.P., Hilley, G.E., 2014. New estimates of silicate weathering rates and their uncertainties in global rivers. *Geochim. Cosmochim. Acta* 134 (2), 257–274.
- Moon, S., Huh, Y., Qin, J., Pho, N., 2007. Chemical weathering in the Hong (Red) River basin: rates of silicate weathering and their controlling factor. *Geochim. Cosmochim. Acta* 71 (6), 1411–1430.
- Nègre, P., Allègre, C.J., Dupre, B., Lewin, E., 1993. Erosion sources determined by inversion of major and trace element ratios and strontium isotopic ratios in river water: the Congo Basin Case. *Earth Planet. Sci. Lett.* 120 (1–2), 59–76.
- Noh, H., Huh, Y., Qin, J., Ellis, A., 2009. Geochemistry of the Three Rivers region of Eastern Tibet. *Geochim. Cosmochim. Acta* 73, 1857–1877.
- Oliva, P., Viers, J., Dupré, B., 2003. Chemical weathering in granitic environments. *Chem. Geol.* 202 (3–4), 225–256.
- Pacheco, F.A.L., Landim, P.M.B., Szocs, T., 2013. Anthropogenic impacts on mineral weathering: a statistical perspective. *Appl. Geochem.* 36 (3), 34–48.
- Probst, A., Gh'ni, A.E., Aubert, D., Fritz, B., McNutt, R., 2000. Strontium as a tracer of weathering processes in a silicate catchment polluted by acid atmospheric inputs, Strengbach, France. *Chem. Geol.* 170 (1–4), 203–219.
- Roy, S., Gaillardet, J., Allègre, C.J., 1999. Geochemistry of dissolved and suspended loads of the Seine River, France: anthropogenic impact, carbonate and silicate weathering. *Geochim. Cosmochim. Acta* 63 (9), 1277–1292.
- Spence, J., Telmer, K., 2005. The role of sulfur in chemical weathering and atmospheric CO₂ fluxes: evidence from major ions, $\delta^{13}\text{C}_{\text{DIC}}$, and $\delta^{34}\text{S}_{\text{SO}_4}$ in rivers of the Canadian Cordillera. *Geochim. Cosmochim. Acta* 69 (23), 5441–5458.
- Stallard, R.F., Edmond, J.M., 1981. Geochemistry of the Amazon 1: precipitation chemistry and the marine contribution to the dissolved load at the time of peak discharge. *J. Geophys. Res.* 86 (C10), 9844–9858.
- Torres, M.A., West, A.J., Li, G., 2014. Sulfuric acid and carbonate dissolution as a source of CO₂ over geological timescales. *Nature* 507 (7492), 346–349.
- Torres, M.A., West, A.J., Clark, K.E., Paris, G., Bouchez, J., Ponton, C., Feakins, S.J., Galy, V., Galy, J.F., 2016. The acid and alkalinity budgets of weathering in the Andes-amazon system: insights into the erosional control of global biogeochemical cycles. *Earth Planet. Sci. Lett.* 450, 381–391.
- Walker, J.C.G., Hays, P.B., Kasting, J.F., 1981. A negative feedback mechanism for the long-term stabilization of Earth's surface temperature. *J. Geophys. Res.* 86, 9776–9782.
- Wallmann, K., 2001. Controls on the Cretaceous and Cenozoic evolution of seawater composition, atmospheric CO₂ and climate. *Geochim. Cosmochim. Acta* 65 (18), 3005–3025.
- Wang, B., Lee, X.-Q., Yuan, H.L., Zhou, H., Cheng, H.G., Cheng, J.Z., Zhou, Z.H., Xing, Y., Fang, B., Zhang, L.K., Fang, Y., 2012. Distinct patterns of chemical weathering in the drainage basins of the Huanghe and Xijiang River, China: evidence from chemical and Sr-isotopic compositions. *J. Asian Earth Sci.* 59 (3), 219–230.
- Wang, L., Zhang, L., Cai, W.J., Wang, B., Yu, Z., 2016. Consumption of atmospheric CO₂ via chemical weathering in the Yellow River basin: the Qinghai-tibet plateau is the main contributor to the high dissolved inorganic carbon in the yellow river. *Chem. Geol.* 430, 34–44.
- Wang, T.J., Jin, L.S., Li, Z.K., Lam, K.S., 2000. A modeling study on acid rain and recommended emission control strategies in china. *Atmos. Environ.* 34 (26), 4467–4477.
- Wang, W., Wang, T., 1996. On acid rain formation in China. *Atmos. Environ.* 30 (23), 4091–4093.
- Wei, G., Ma, J., Liu, Y., Xie, L., Lu, W., Deng, W., Ren, Z., Zeng, T., Yang, Y., 2013. Seasonal changes in the radiogenic and stable strontium isotopic composition of Xijiang River water: implications for chemical weathering. *Chem. Geol.* 343 (3), 67–75.
- White, A.F., Blum, A.E., 1995. Effects of climate on chemical weathering in watersheds. *Geochim. Cosmochim. Acta* 59 (9), 1729–1747.
- Wu, W., 2016. Hydrochemistry of inland rivers in the north Tibetan Plateau: constraints and weathering rate estimation. *Sci. Total Environ.* 541, 468–482.
- Wu, W., Xu, S., Yang, J., Yin, H., 2008. Silicate weathering and CO₂ consumption deduced from the seven Chinese rivers originating in the Qinghai-Tibet Plateau. *Chem. Geol.* 249, 307–320.
- Xu, Y., Duan, N., Chai, F., Hu, X., Li, H., Weng, J., 2006. Numerical simulation of sulfur deposition in China. *Res. Environ. Sci.* 19(5), 1–10 (in Chinese, with English Abstr.).
- Xu, Z., Liu, C.-Q., 2007. Chemical weathering in the upper reaches of Xijiang River draining the Yunnan-Guizhou Plateau, Southwest China. *Chem. Geol.* 239 (1), 83–95.
- Xu, Z., Liu, C.-Q., 2010. Water geochemistry of the Xijiang basin rivers, South China: chemical weathering and CO₂ consumption. *Appl. Geochem.* 25 (10), 1603–1614.
- Xu, Z., Shi, C., Tang, Y., Han, H.Y., 2011. Chemical and strontium isotopic compositions of the Hanjiang Basin Rivers in China: anthropogenic impacts and chemical weathering. *Aquat. Geochem.* 17 (3), 243–264.
- Yoshimura, K., Nakao, S., Noto, M., Inokura, Y., Urata, K., Chen, M., Lin, P.W., 2001. Geochemical and stable isotope studies on natural water in the Taroko Gorge karst area, Taiwan-chemical weathering of carbonate rocks by deep source CO₂ and sulfuric acid. *Chem. Geol.* 177 (3–4), 415–430.
- Yuan, D., 1991. *Karst of China*. Geological Publishing House, Beijing, China (in Chinese).
- Zhang, S.R., Lu, X.X., Higgitt, D.L., Chen, C.T.A., Sun, H.G., Han, J.T., 2007. Water chemistry of the Zhujiang (Pearl River): natural processes and anthropogenic influences. *J. Geophys. Res.* 112 (F1), 137–161.